Laser-induced damage of nonlinear crystals in ultrafast, high-repetition-rate, mid-infrared optical parametric amplifiers pumped at 1 µm

Mark Mero*[a], Li Wang[a], Weidong Chen[a,b], Ning Ye[b], Ge Zhang[b], Valentin Petrov[a], Zsuzsanna Heiner[§c]

[a]Max Born Institute for Nonlinear Optics and Short Pulse Spectroscopy, 12489 Berlin, Germany; [b]Key Laboratory of Optoelectronic Materials Chemistry and Physics, Fujian Institute of Research on the Structure of Matter, Chinese Academy of Sciences, Fuzhou, 350002 China; [c]School of Analytical Sciences Adlershof SALSA, Humboldt-Universität zu Berlin, 12489 Berlin, Germany

ABSTRACT

The exceptional power scalability of Yb lasers has enabled the development of pulsed optical parametric amplifiers (OPA's) operating at the short-wave edge of the mid-IR (MIR) with average powers beyond 10 W simultaneously providing peak powers in excess of 1 GW. Further wavelength extension into the longer-wave MIR is enabled by novel wide-bandgap non-oxide nonlinear crystals that can be pumped directly at 1 µm without detrimental one- and two-photon absorption of pump radiation. Eliminating the usual difference frequency generation step in producing MIR pulses above 5 µm could potentially increase the conversion efficiency of parametric down-conversion devices and enable a significant boost in the attainable average and peak power. Despite their utmost importance, material properties related to ultrafast laser-induced damage in nonlinear crystals are rarely investigated in the corresponding laser parameter range. In order to help unravel the complicated interplay of photorefractive effects, thermal lensing, and self-focusing/defocusing affecting the beam quality and catastrophic breakdown threshold in MIR OPA's, we present the nonlinear index of refraction at 1 µm of $KTiOAsO_4$, $LiGaS_2$, and $BaGa_4S_7$. The reported data provide crucial design parameters for the development of high-average-power MIR OPA's. As examples, (i) a 100-kHz, 1.55/3.1 µm dual-beam OPA delivering multi-GW peak power in each beam and a total average power of 55 W and (ii) a 100-kHz, sub-100-fs, 1-µm-pumped OPA tunable in the 5.7-10.5-µm range are briefly presented.

Keywords: Nonlinear optical crystals, laser-induced damage, photorefractive damage, z-scan, nonlinear refractive index, $KTiOAsO_4$ (KTA), $LiGaS_2$ (LGS), $BaGa_4S_7$ (BGS)

1. INTRODUCTION

Technologically mature, diode-pumped picosecond and sub-picosecond Yb lasers are gradually replacing Ti:sapphire laser systems and becoming the main workhorses behind applications requiring simultaneously high peak and average power. The rapidly expanding field of strong-field spectroscopy and table-top secondary source development utilizing high-harmonic generation can greatly benefit from frequency down-conversion of the output of Yb lasers to ultrashort short-wave and mid-wave infrared (MIR, 3-30 µm) pulses. A well-established route to efficient frequency down-conversion that also supports few-cycle pulse durations employs optical parametric amplifiers (OPA's) based on nonlinear optical crystals. Despite their utmost importance, properties of nonlinear optical crystals affecting ultrafast laser-induced damage at repetition rates above a few kHz are rarely considered in the OPA design or investigated. Depending on the choice of crystal, such material properties include two-photon absorption coefficients at the ~1.0-µm pump wavelength, green and blue light induced infrared absorption, insufficient heat conductivity resulting in a temperature gradient due to residual single-photon and two-photon absorption of the pump laser beam and/or optical single- or multi-phonon absorption of the infrared signal/idler beams, susceptibility to photorefractive damage, and the anisotropic nonlinear refractive index leading to self- and cross-phase modulation.

*mero@mbi-berlin.de,[§]heinerzs@hu-berlin.de

For OPA's operating up to ~4 μm, various wide-bandgap oxide nonlinear optical crystals are available commercially with aperture sizes well above 1 cm that can be pumped by ultrashort 1-μm pump lasers with negligible two-photon absorption and high damage threshold: $LiNbO_3$, $KNbO_3$, and $KTiOAsO_4$ (KTA). Compared to $LiNbO_3$ and $KNbO_3$, KTA is a superior nonlinear optical material regarding resistance to laser-induced damage, photodarkening, photorefractive effects, and OH absorption at ~2.8 μm.[1-4] As oxide crystals exhibit strong multi-phonon absorption above 5 μm, one typically employs an OPA-DFG (difference frequency generation) cascade to reach this wavelength range, where the OPA utilizes oxide crystals and the DFG stage is based on a narrow-bandgap non-oxide semiconductor crystal. Such crystals include $AgGaSe_2$ or GaSe, which exhibit high nonlinear coefficients, but cannot be pumped by $\lesssim$ 1.5-ps, ~1-μm pulses without inducing two-photon absorption or damage. The overall pump-to-MIR energy conversion efficiency of such a cascade is < 0.5% at a center wavelength of ~8 μm. Removal of the DFG step can potentially increase the conversion efficiency. However, there are only a limited number of non-oxide crystals that are both highly transparent at wavelengths above 5 μm and have sufficiently large damage threshold and bandgap. $LiGaS_2$ (LGS) and $BaGa_4S_7$ (BGS) are relatively new, promising non-oxide crystals[5,6] that can potentially satisfy the aforementioned requirements of high-average-power, 1-μm-pumped MIR OPA's in the 5-9 μm range albeit at much lower figures of merit compared to the narrow-bandgap alternatives, in particular the commercially available $AgGaS_2$ which shows a similar transmission range.

In Refs.[7,8], we reported the catastrophic breakdown threshold induced by ≤ 1.3-ps, 1-μm laser pulses of various blank and periodically-poled $LiNbO_3$ and blank Rb-doped $KTiOPO_4$ (RKTP) crystals as a function of laser repetition rate and pulse duration. As the damage threshold intensity increases with decreasing pulse duration, self-focusing effects become more noticeable complicating the extraction of the intrinsic damage threshold even at a crystal thickness of only 2 mm. In addition, onset of photorefractive processes for both materials occurs well below the catastrophic breakdown threshold. As a first step in unraveling the interplay of the various processes, information on the nonlinear refractive index, n_2, is needed. Thermal lensing[9] and cascaded $\chi^{(2)}$: $\chi^{(2)}$ processes[10] can contribute to the effective n_2, which is an important parameter from the perspective of OPA development. Therefore, measurement of the nonlinear refractive index at the relevant OPA crystal-cut and laser polarization is required ideally as a function of laser repetition rate. The n_2 value of KTA was reported only for z-cut samples[11] at a wavelength and repetition rate of 780 nm and 76 MHz, respectively. Experimental data on the nonlinear refractive index of LGS and BGS have not been published yet.

Here, we report the results of z-scan measurements of the effective nonlinear refractive index of KTA, LGS, and BGS crystals cut for mid-infrared optical parametric amplification at a pump wavelength of 1 μm. In addition, we briefly describe the 100-kHz MIR OPA systems, where the results of the n_2 measurements were included in the design.

2. METHODS

2.1 Samples

In order to benchmark our z-scan measurements, we chose sample materials with well-known n_2 values: L = 1-mm-long uncoated fused silica and ZnSe (polycrystalline) windows.

The KTA sample was an anti-reflection coated, 4-mm-long crystal cut at $\theta = 42^o$, $\phi = 0^o$ for type II optical parametric amplification in the XZ plane at extraordinary 1.55-μm signal polarization.

The LGS sample was an uncoated, 5-mm-long crystal cut at $\theta = 48.2^o$, $\phi = 0^o$ for type I optical parametric amplification in the XZ plane.

The BGS samples were uncoated, 4.8-mm-long crystals with unknown orientation. Based on conoscopic measurements, the crystals were either X- or Z-cut samples.

All three crystals are orthorhombic (*mm*2 point group) and XYZ designate the dielectric frame according to $n_X < n_Y < n_Z$.

2.2 Z-scan measurement

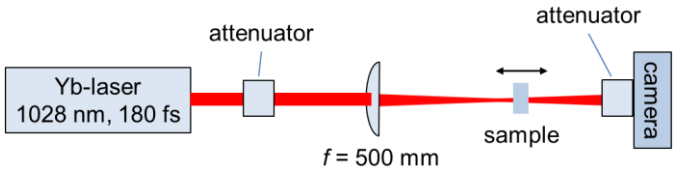

Figure 1. Scheme of z-scan measurements.

The scheme of our z-scan setup is shown in Fig. 1. We employed a commercial Yb laser delivering 1.03-µm, 60-µJ, 180-fs pulses at an adjustable repetition rate up to 100 kHz. The temporal profile of the pulses was characterized using second-harmonic generation frequency resolved optical gating. The retrieved temporal profile was included in the model equation of the z-scan traces. The pulses were focused on the sample by an f = 500 mm singlet lens to a beam waist radius of w_0 = 65 µm. The M^2 values in the horizontal and vertical planes were measured to be ≤ 1.1 at negligible astigmatism using a commercial beam quality characterization system. We conducted z-scans at repetition rates of (i) 100 Hz where thermo-optic effects were expected to be negligible and (ii) 100 kHz, which was the target repetition rate in our two < 4-µm and > 5-µm MIR OPA designs. Instead of using photodiodes, we employed a camera to record the far-field profile of the beam that was transmitted through the sample and extracted the open-aperture and closed-aperture traces by analyzing the images. The closed-aperture transmittance (T) traces were fitted using the equation valid in the thin-sample limit,[12]

$$T(x,\langle\Delta\varphi_0\rangle) = 1 - [4x\langle\Delta\varphi_0\rangle]/[(x^2+9)(x^2+1)], \quad (1)$$

where $x = z/z_0$ is the normalized translation position, z_0 is the Rayleigh range, and $\langle\Delta\varphi_0\rangle$ is the time-averaged phase change. We determined the n_2 values by either obtaining a fit value for $\langle\Delta\varphi_0\rangle$ based on Eq. (1) or using the expression relating it to the difference between the normalized peak and valley transmittance,

$$\langle\Delta\varphi_0\rangle = \Delta T_{v\text{-}p} / [0.406\ (1\text{-}S)^{0.25}], \quad (2)$$

valid for small phase shifts.[12] Here S denotes the linear aperture transmission. The corresponding extracted nonlinear refractive indices are denominated as either n_2(fit) or $n_2(\Delta T_{v\text{-}p})$, respectively. The relationship between the time-averaged phase shift and the nonlinear index of refraction reads,

$$n_2 \cong \langle\Delta\varphi_0\rangle\ (0.39\lambda w_0^2 \tau_p) / (L_{eff}\, E_{int}), \quad (3)$$

where λ is the center wavelength, τ_p is the pulse duration at full width at half maximum, E_{int} is the pulse energy inside the material, and $L_{eff} \approx L$ (sample length) at negligible linear absorption. The numerical factor 0.39 was obtained by taking the actual temporal profile into account.

3. RESULTS

3.1 Nonlinear refractive index of reference samples

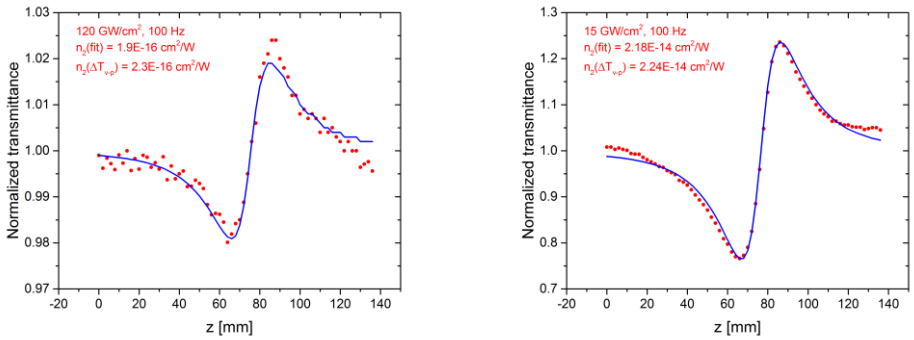

Figure 2. Closed-aperture z-scan traces of the fused silica (left) and ZnSe (right) samples, recorded at a laser repetition rate of 100 Hz and at peak on-axis intensities of 120 GW/cm^2 and 15 GW/cm^2, respectively.

We obtained n_2 = 2.3×10^{-16} cm^2/W and 2.2×10^{-14} cm^2/W for fused silica and ZnSe, respectively (cf. Fig. 2), in close agreement with the literature.[13,14]

3.2 Nonlinear refractive index of KTA

In Ref.[11], the nonlinear refractive index of KTA was measured only for Z-cut samples and at a very high repetition rate (i.e., 76 MHz) yielding a value n_2 = 1.7×10^{-15} cm^2/W. In order to cross-check possible thermo-optic, $\chi^{(2)}$: $\chi^{(2)}$, and photorefractive effects, we recorded z-scan traces both at 100 Hz and 100 kHz for a crystal cut for MIR optical parametric amplification. Figure 3 shows the results obtained at 100 Hz for laser polarization in the XZ plane and parallel to the Y axis. We obtained $n_2 \approx$ 1.5×10^{-15} cm^2/W equal within error bars for both laser polarizations. The extracted values were approximately constant in the peak intensity range of 15-60 GW/cm^2 (cf. Fig. 4). At 100 kHz and peak intensities above 60 GW/cm^2, we observed diffraction effects, possibly due to photorefractive damage, that distorted the z-scan traces and resulted in strong scattering in a large solid angle. With the laser beam blocked, the beam recovered within seconds to the original, undistorted profile. The right panel of Fig. 4 demonstrates the onset of photorefractive effects by showing the transmitted far-field (i.e., $z >> z_0$) beam profiles at different peak intensities and repetition rates at the sample translation position corresponding to the minimum in the closed-aperture transmittance traces.

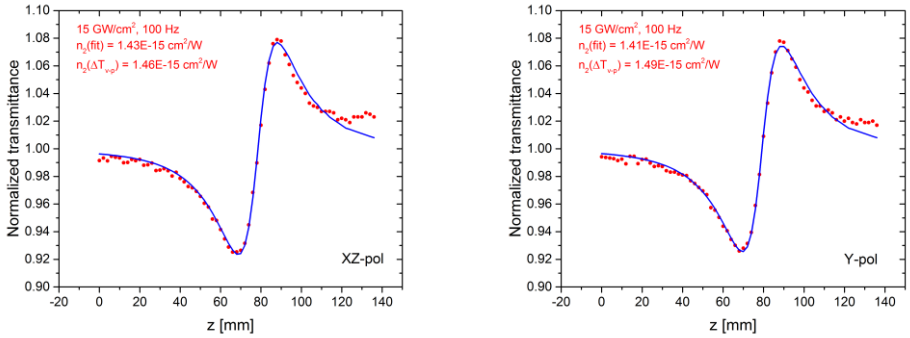

Figure 3. Closed-aperture z-scan traces of the KTA sample, recorded at a laser polarization in the XZ plane (left) and parallel to the Y-axis (right). The laser repetition rate and peak intensity was 100 Hz and 15 GW/cm^2, respectively. The red circles are experimental data points, while the blue lines are fit curves based on Eq. (1).

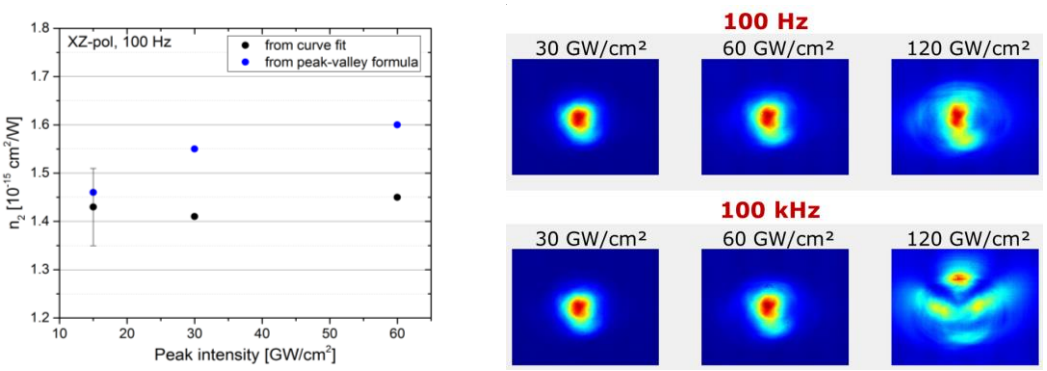

Figure 4. Left: n_2 values extracted from closed-aperture z-scan traces of the KTA samples, recorded with laser polarization in the XZ plane at different peak intensities at 100 Hz. The error bar at 15 GW/cm^2 is the standard deviation of fit values obtained for three z-scan data sets. Right: transmitted far-field beam profiles at different peak intensities and repetition rates at the sample translation position corresponding to the minimum in the closed-aperture transmittance traces.

3.3 Nonlinear refractive index of LGS

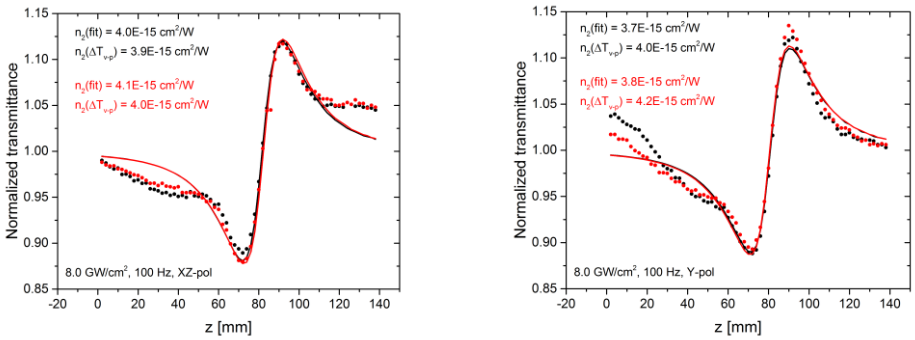

Figure 5. Closed-aperture z-scan traces of the LGS sample at a laser polarization in the XZ-plane (left) and parallel to the Y-axis (right). The peak intensity and the repetition rate were 8.0 GW/cm^2 and 100 Hz, respectively. The different colors mean different z-scan measurement runs.

Figure 5 shows the z-scan traces we obtained for LGS for two orthogonal laser polarizations at a repetition rate of 100 Hz and a peak, on-axis intensity of 8.0 GW/cm^2. We obtained $n_2 \approx 4.1\times10^{-15}$ cm^2/W, which was only very weakly dependent on laser polarization. The nonlinear refractive index did not change when increasing the repetition rate from 100 Hz to 100 kHz and keeping the peak intensity constant at 8.0 GW/cm^2 (cf. Fig. 6).

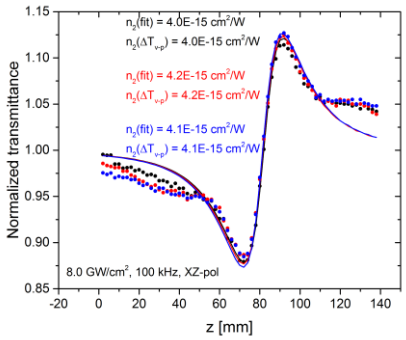

Figure 6. Closed-aperture z-scan traces of the LGS sample at a laser polarization in the XZ-plane. The peak intensity and the repetition rate were 8.0 GW/cm^2 and 100 kHz, respectively. The different colors mean different z-scan measurement runs.

3.4 Nonlinear refractive index of BGS

The left panel in Fig. 7 shows the z-scan traces we obtained for BGS for two orthogonal laser polarizations at a repetition rate of 100 Hz and a peak, on-axis intensity of 8.0 GW/cm^2. We obtained $n_2 \approx 7.6\times10^{-15}$ cm^2/W and 8.3×10^{-15} cm^2/W, depending on laser polarization. The weak polarization dependence was reproducible from day to day. The nonlinear refractive index did not change when increasing the repetition rate from 100 Hz to 100 kHz and keeping the peak intensity constant at 8.0 GW/cm^2 (cf. Fig. 6).

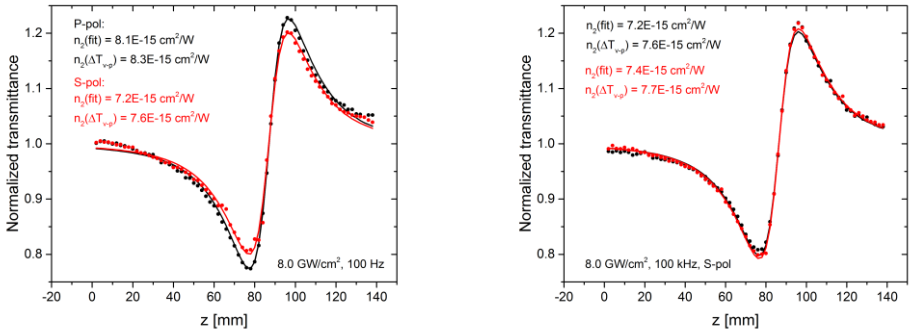

Figure 7. Closed-aperture z-scan traces of the BGS samples at two, orthogonal laser polarizations denoted by p-pol and s-pol. The repetition rate was 100 Hz (left) and 100 kHz (right). The peak intensity was 8.0 GW/cm^2.

4. MIR OPA EXAMPLES

4.1 High-average-power OPA system based on KTA

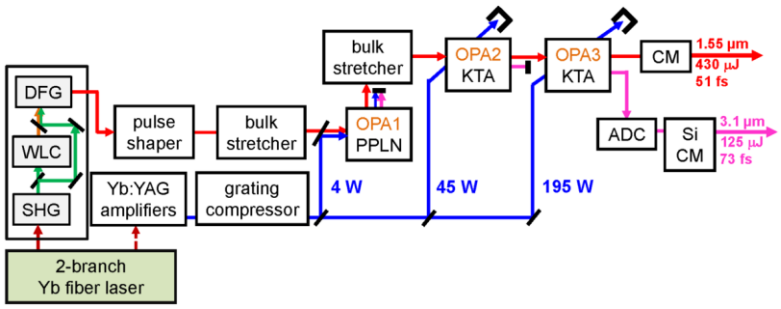

Figure 8. Scheme of 100-kHz MIR OPA system. Fig. 1 from Ref.[17] was reused (https://doi.org/10.1364/OL.43.005246 , licensed under CC BY 4.0). No changes were made to the figure.

Bulk $KNbO_3$-based and $LiNbO_3$-based power OPA's were shown to deliver 19 W of average power at 160 kHz in 97 fs pulses[15] and 15 W of average power in 42 fs pulses[16] at 3.25 and 3.1 µm, respectively. Based on our tests on a small-scale 100-kHz, 1.5/3.2-µm OPA system, we found that KTA booster amplifiers vastly outperform periodically-poled $LiNbO_3$–based OPA's even at low average powers.[17] Therefore, KTA was chosen for the high-power booster amplifiers at the Max Born Institute. Figure 8 displays the architecture of our dual-beam, high-average-power OPA delivering a total average power of 55 W at 1.55 and 3.1 µm at a repetition rate of 100 kHz.[18] The second and third booster OPA's are based on a 4 and a 2-mm-long KTA crystal, both pumped at a peak intensity of 70 GW/cm^2. The OPA design took into account the nonlinear refractive index of KTA and thermal lensing supplied by our z-scan studies. The choice of pump peak intensities and wavefront curvatures ensures stable long-term operation with high beam quality of both infrared output beams.[18]

4.2 High-repetition-rate OPA system based on LGS

Aided by our z-scan studies, a pump intensity of 45 GW/cm^2 at an appropriately diverging wavefront was chosen for the 180-fs, 1.03-µm, 100-kHz pump pulse train to ensure long-term-stable operation. We obtained the first sub-100-fs pulses near 8 µm from a 1-µm-pumped LGS OPA, corresponding to sub-4 optical cycles. The overall pump-to-8-µm energy conversion efficiency of our OPA exceeded that of OPA-DFG-based schemes by a more than a factor of 3. The LGS crystal showed no sign of deterioration over extended periods of time and the OPA was successfully integrated in the first 100-kHz vibrational sum-frequency generation spectrometer covering the 5.7-10.5-µm spectral range in the chemically important molecular fingerprint region.[19]

5. CONCLUSIONS

When pumped at repetition rates >> 10 kHz and pulse durations ≤ 1 ps, intrinsic catastrophic laser-induced breakdown thresholds of OPA crystals are difficult to extract. Thermal lensing, non-permanent photorefractive damage, n_2 effects, and strong-field electronic excitation mechanisms act simultaneously. Therefore, the measured incident damage threshold values are only extrinsic values dependent on wavefront curvature, sample length, pulse duration, and beam size. Importantly, catastrophic breakdown is preceded by photorefractive, thermal, and n_2 effects, which all tend to deteriorate OPA performance. As a result, OPA's in the above pulse parameter range are expected to operate well below the catastrophic breakdown threshold; at a pump intensity level, where thermo-optic and Kerr-lensing effects need to be taken into account in the OPA design. We presented effective n_2 values of KTA and two novel, wide-gap non-oxide crystals, $LiGaS_2$ and $BaGa_4S_7$, the latter of which holds great promise for power-scalable OPA's in the 5-9 µm spectral range.

ACKNOWLEDGMENTS

We gratefully acknowledge funding from the European Union's Horizon 2020 research and innovation programme under grant agreement no. 654148 Laserlab-Europe, the Deutsche Forschungsgemeinschaft (DFG) grant no. GSC 1013 SALSA and PE 607/14-1, and the Joint Sino-German Research Projects: the National Natural Science Foundation of China (NSFC) and the Deutsche Forschungsgemeinschaft (DFG), NSFC-DFG No. 51761135115. Z.H. acknowledges funding by a Julia Lermontova Fellowship from DFG, No. GSC 1013 SALSA.

REFERENCES

[1] Lin., S., Tanaka, Y., Takeuchi, S., and Suzuki, T., "Improved dispersion equation for MgO:$LiNbO_3$ crystal in the infrared spectral range derived from sum and difference frequency mixing" IEEE J. Quantum Electron. 32(1), 124-126 (1996).

[2] Umemura, N., Yoshida, K., and Kato, K., "Phase-matching properties of $KNbO_3$ in the mid-infrared," Appl. Opt. 38(6), 991-994 (1999).

[3] Hansson, G., Karlsson, H., Wang, S., and Laurell, F., "Transmission measurements in KTP and isomorphic compounds," Appl. Opt. 39(27), 5058-5069 (2000).

[4] Mero, M., Noack, F., Bach, F., Petrov, V., and Vrakking, M. J. J., "High-average-power, 50-fs parametric amplifier front-end at 1.55 µm," Opt. Express 23(26), 33157-33163 (2015).

[5] Isaenko, L., Yelisseyev, A., Lobanov, S., Krinitsin, P., Petrov, V., and Zondy, J.-J., "Ternary chalcogenides $LiBC_2$ (B = In,Ga; C = S,Se,Te) for mid-IR nonlinear optics," J. Non-Cryst. Solids 352(23-25), 2439–2443 (2006).

[6] Badikov, V., Badikov, D., Shevyrdyaeva, G., Tyazhev, A., Marchev, G., Panyutin, V., Noack, F., Petrov, V., and Kwasniewski, A., "$BaGa_4S_7$: wide-bandgap phase-matchable nonlinear crystal for the mid-infrared" Opt. Mater. Express 1(3), 316-320 (2011).

[7] Bach, F., Mero, M., Chou, M.-H., and Petrov, V., "Laser induced damage studies of $LiNbO_3$ using 1030-nm, ultrashort pulses at 10-1000 kHz," Opt. Mater. Express 7(1), 240-252 (2017).

[8] Bach, F., Mero, M., Pasiskevicius, V., Zukauskas, A., and Petrov, V., "High repetition rate, femtosecond and picosecond laser induced damage thresholds of Rb:$KTiOPO_4$ at 1.03 µm," Opt. Mater. Express 7(3), 744-750 (2017).

[9] Falconieri, M., "Thermo-optical effects in z-scan measurements using high-repetition-rate lasers," J. Opt. A: Pure Appl. Opt. 1(6), 662–667 (1999).

[10] DeSalvo, R., Hagan, D. J., Sheik-Bahae, M., Stegeman, G., and Van Stryland, E. W., "Self-focusing and self-defocusing by cascaded second-order effects in KTP," Opt. Lett. 17(1), 28-30 (1992).

[11] Li, H. P., Kam, C. H., Lam, Y. L., and Ji, W., "Femtosecond z-scan measurements of nonlinear refraction in nonlinear optical crystals," Opt. Mater. 15(4), 237-242 (2001).

[12] Sheik-Bahae, M., Said, A. A., Wei, T.-H., Hagan, D. J., and Van Stryland, E. W., "Sensitive measurement of optical nonlinearities using a single beam," IEEE J. Quantum Electron. 26(4), 760-769 (1990).

[13] Slavinskis, N., Murauskas, and E., Dement'ev, A. S., "Dependence of Z-scan measurements on the spatiotemporal pulse parameters," Lithuanian J. Phys. 51(2), 127-135 (2011).
[14] Said, A. A., Sheik-Bahae, M., Hagan, D. J., Wei,T. H., Wang, J., Young, J. and Van Stryland, E. W., "Determination of bound-electronic and free-carrier nonlinearities in ZnSe, GaAs, CdTe, and ZnTe," J. Opt. Soc. Am. B 9(3), 405-414 (1992).
[15] Elu, U., Baudisch, M., Pires, H., Tani, F., Frosz, M. H., Köttig, F., Ermolov, A., Russell, P. St. J., and Biegert, J., "High average power and single-cycle pulses from a mid-IR optical parametric chirped pulse amplifier," Optica 4(9), 1024-1029 (2017).
[16] Thiré, N., Maksimenka, R., Kiss, B., Ferchaud, C., Gitzinger, G., Pinoteau, T., Jousselin, H., Jarosch, S., Bizouard, P., Di Pietro, V., Cormier, E., Osvay, K., and Forget, N., "Highly stable, 15 W, few-cycle, 65 mrad CEP-noise mid-IR OPCPA for statistical physics," Opt. Express 26(21), 26907-26915 (2018).
[17] Heiner, Z., Petrov, V., Steinmeyer, G., Vrakking, M. J. J., and Mero, M., "100-kHz, dual-beam OPA delivering high-quality, 5-cycle angular-dispersion-compensated mid-infrared idler pulses at 3.1 μm," Opt. Express 26(20), 25793-25804 (2018).
[18] Mero, M., Heiner, Z., Petrov, V., Rottke, H., Branchi, F., Thomas, G. M., and Vrakking, M. J. J., "43 W, 1.55 μm and 12.5 W, 3.1 μm dual-beam, sub-10 cycle, 100 kHz optical parametric chirped pulse amplifier," Opt. Lett. 43(21), 5246-5249 (2018).
[19] Heiner, Z., Wang, L., Petrov, V., and Mero, M., "Broadband vibrational sum-frequency generation spectrometer at 100 kHz in the 950-1750 cm^{-1} spectral range utilizing a $LiGaS_2$ optical parametric amplifier," Opt. Express 27(11), 15289-15297 (2019).

Title:

Laser-induced damage of nonlinear crystals in ultrafast, high-repetition-rate, mid-infrared optical parametric amplifiers pumped at 1 μm

Authors:

Mark Mero, Li Wang, Weidong Chen, Ning Ye, Ge Zhang, Valentin Petrov, Zsuzsanna Heiner

Manuscript

The original publication may be found at:

Journal: Proc. SPIE 11063, Pacific Rim Laser Damage 2019: Optical Materials for High-Power Lasers, 1106307 (8 July 2019)

DOI: https://doi.org/10.1117/12.2540125